

Antimatter and Matter Production in Heavy Ion Collisions at CERN (The NEWMASS Experiment NA52)

K. Pretzl for the NA52 collaboration:

G. Ambrosini¹, R. Arsenescu¹, C. Baglin², H.P. Beck¹, K. Borer¹,
A. Bussière², K. Elsener³, Ph. Gorodetzky⁵, J.P. Guillaud²,
P. Hess¹, S. Kabana¹, R. Klingenberg¹, G. Lehmann¹, T. Lindén⁴,
K.D. Lohmann³, R. Mommsen¹, U. Moser¹, K. Pretzl¹, J. Schacher¹,
R. Spiwoks¹, F. Stoffel¹, J. Tuominiemi⁴, M. Weber¹

¹ Laboratory for High Energy Physics, University of Bern, Sidlerstrasse 5, CH-3012
Bern, Switzerland

² CNRS-IN2P3, LAPP Annecy, F-74941 Annecy-le-Vieux, France

³ CERN, SL Division, CH-1211 Geneva 23, Switzerland

⁴ Dept. of Physics, University of Helsinki, PO Box 9, FIN-00014 Helsinki, Finland

⁵ PCC - Collège de France, 11 Place Marcellin Berthelod, 75005 Paris, France

Abstract. Besides the dedicated search for strangelets NA52 measures light (anti)particle and (anti)nuclei production over a wide range of rapidity. Compared to previous runs the statistics has been increased in the 1998 run by more than one order of magnitude for negatively charged objects at different spectrometer rigidities. Together with previous data taking at a rigidity of -20 GeV/c we obtained 10^6 \bar{p} , 10^3 \bar{d} and two ${}^3\bar{\text{He}}$ without centrality requirements. We measured nuclei and antinuclei (p, d, \bar{p}, \bar{d}) near midrapidity covering an impact parameter range of $b \sim 2-12$ fm. Our results strongly indicate that nuclei and antinuclei are mainly produced via the coalescence mechanism. However the centrality dependence of the antibaryon to baryon ratios show that antibaryons are diminished due to annihilation and breakup reactions in the hadron dense environment. The volume of the particle source extracted from coalescence models agrees with results from pion interferometry for an expanding source. The chemical and thermal freeze-out of nuclei and antinuclei appear to coincide with each other and with the thermal freeze-out of hadrons.

1. Introduction

NA52 is a fixed target experiment at the CERN SPS looking at 158 A GeV/c Pb-Pb collisions. We identify single particles near $p_{\perp} = 0$. Our apparatus is sensitive to all objects reaching the trigger counter located $0.9\mu\text{s} \cdot c$ behind the target. Besides the dedicated search for strangelets [1, 2, 3, 4, 5] we measure (anti)particle and (anti)nuclei over a wide range of rapidity [5, 6, 7, 8, 9, 10, 11, 12]. We have recorded $10^6 \bar{p}$, $10^3 \bar{d}$ and two $\overline{{}^3\text{He}}$ at a spectrometer rigidity of $-20 \text{ GeV}/c$. No antitriton has been observed. This finds its explanation in the factor of four smaller acceptance for a singly charged particle like the triton as compared to a doubly charged particle like the $\overline{{}^3\text{He}}$, with approximately the same production cross section.

In the present paper we focus on features of baryon, antibaryon as well as nuclei and antinuclei production in Pb+Pb collisions at 158 A GeV. A general description of the experimental setup can be found in [5, 11, 12, 13]. The m_T and rapidity dependence of baryons and antibaryons and their comparison to coalescence and thermodynamical model predictions and to p+Be collisions at 220 GeV, are shown here for the first time. Antimatter production in heavy ion collisions, may give important experimental information on the event of the QCD phase transition of deconfined quarks and gluons to confined hadrons [14]. The discovery of the latter is an outstanding goal of the heavy ion physics experiments [15].

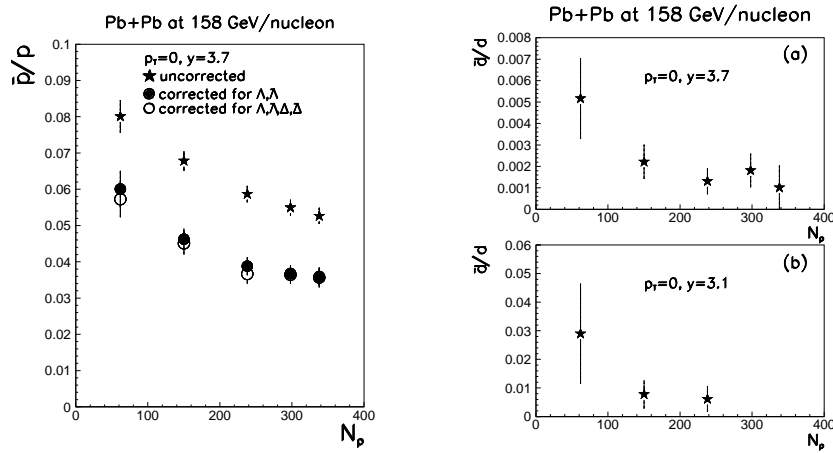


Fig. 1. Dependence of the \bar{p}/p (left) and the \bar{d}/d (right) ratios from the mean number of participant nucleons in Pb+Pb collisions at 158 A GeV near zero p_T . The Λ and Δ correction is performed using VENUS 4.12 [32]

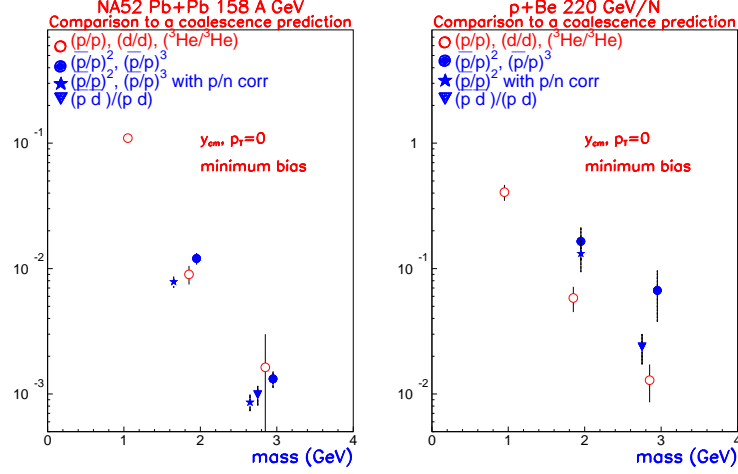


Fig. 2. Antiparticle to particle ratios near zero transverse momentum and at midrapidity, compared to a coalescence model prediction as a function of particle mass. Left: data from Pb+Pb collisions at 158 GeV per nucleon (NA52). Right: data from p+Be collisions at 220 GeV [33]. All data are minimum bias. See text for explanation.

2. Results and discussion

Antibaryon production is expected to be enhanced in a collision which goes through the QCD phase transition, as compared to one which does not [14]. However a possible enhancement can be counterbalanced by the effect of annihilation of antibaryons in the baryon rich environment during the course of a collision of heavy nuclei like lead [16]. In lead lead collisions at $\sqrt{s}=17$ GeV, baryons are stopped enough to populated significantly the central rapidity region [7].

The centrality dependence of particle, antiparticle and baryon, antibaryon yields has previously been investigated by the NA52 experiment and is published in [7, 12]. A comparison of our data to the results of other experiments can be found in [17].

In Fig. 1 our data on \bar{p}/p and \bar{d}/d ratios as a function of centrality are shown. Throughout this paper the shown errorbars correspond to statistical errors only, unless stated differently. The systematic error which is mainly due to uncertainties in the acceptance of the spectrometer is estimated to be 20%. The observed decrease of both ratios with increasing centrality of the collision can be understood as a result of increasing annihilation of antibaryons in a baryon rich environment of a central collision.

However this effect may also be connected to the low p_T acceptance of our spectrometer. Preliminary analysis of other measurements at full p_T and in a similar centrality range show no significant decrease of the \bar{p}/N ratio with centrality [18]. It is conceivable that near zero p_T the baryon density is higher than at larger p_T values, due to many projectile fragments, which acquire a very small p_T kick, but populate a large range in rapidity. These small angle protons can induce a larger annihilation of the antiprotons which are produced near zero p_T .

At the moment it is not possible to speak about antibaryon enhancement in the investigated collisions, because the effect of annihilation has not yet been quantified. NA52 took data in 1998 with the goal to measure the effect of antibaryon annihilation through measurements of anisotropic distributions of antibaryons in and out of the 'event plane' (see [6] for first results).

Other questions which arise are how and when are the nuclei and antinuclei produced in the course of the collision, and what can we learn from their properties. We investigate first their production mechanism. Besides direct pair production, nuclei and antinuclei can also be produced by coalescence of p, n, \bar{p}, \bar{n} and of other light nuclei and antinuclei. But also other mechanisms like collective antimatter production in analogy to spontaneous positron emission and vacuum decay processes in QED may play a role [19]. Furthermore, nuclei can originate from projectile/target fragmentation which, although they peak at beam/target rapidity and zero p_t , can populate the whole rapidity region due to stopping.

We address the question if coalescence is the dominant production mechanism by comparing the \bar{d}/d and ${}^3\bar{He}/{}^3He$ ratios with simple coalescence model predictions using the data themselves, namely we examine if the following conditions for the yield ratios hold:

$$\begin{aligned} (\bar{p}/p)^2 &\sim \bar{d}/d \\ (\bar{p}/p)^3 &\sim {}^3\bar{He}/{}^3He \\ (\bar{p}\bar{d})/(pd) &\sim {}^3\bar{He}/{}^3He. \end{aligned}$$

The results are shown in figure 2. We assumed that the number of n, \bar{n} is equal to the number of p, \bar{p} . An exception are the points noted as 'with p/n correction' where we include a correction to the number of neutrons using $n = p \cdot (A - Z/Z)$. This correction accounting for the number of protons and neutrons in the target and projectile nuclei is not necessarily correct since the ratio n/p may change in the course of the collision. The coalescence prediction agrees with the Pb+Pb data at 158 A GeV (figure 2 (left)), while it does not describe so well the p+Be data at 220 GeV (figure 2 (right)). Both data sets are minimum bias, at $p_T \sim 0$ and at midrapidity. Figure 2 suggests that coalescence is the dominant production mechanism for nuclei and antinuclei in Pb+Pb collisions, while in p+Be collisions nucleon and antinucleon pairs seem to be produced more directly and are less affected by annihilation processes and breakup.

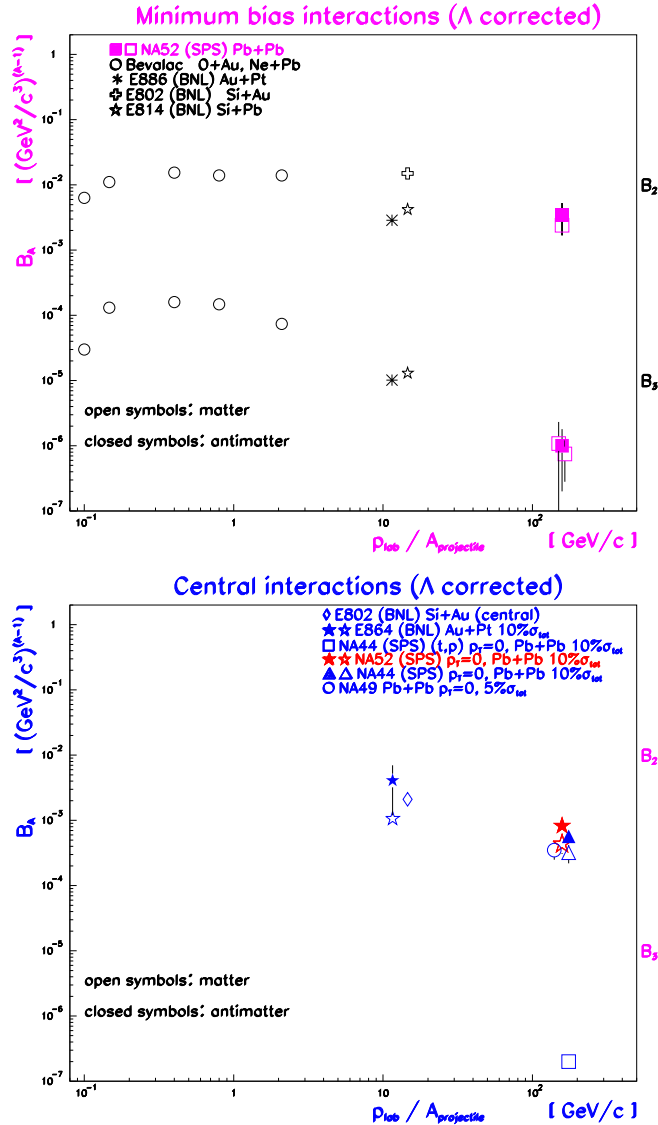


Fig. 3. Compilation of coalescence scaling factors at different momentum per nucleon of the incident projectile. The above figure shows data taken with minimum bias trigger (all impact parameters), the one below with central trigger (small impact parameters, typically 5-10% of σ_{tot}). The d/p^2 and \bar{d}/\bar{p}^2 data (B_2) of NA52 are corrected for Λ and $\bar{\Lambda}$ decays.

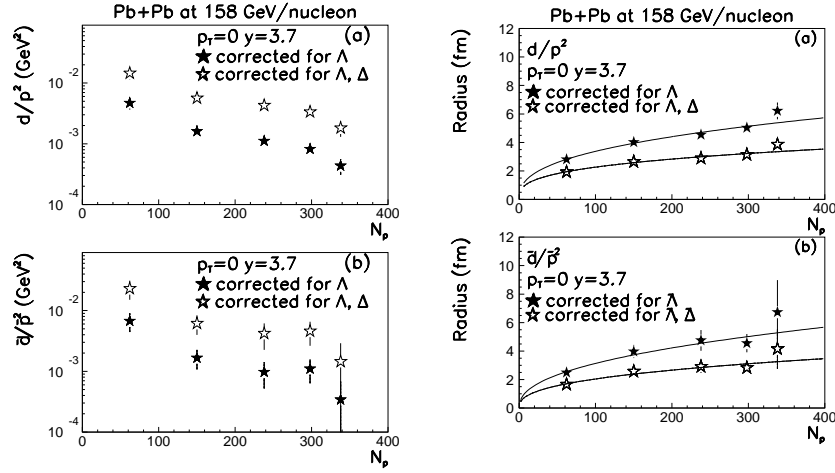


Fig. 4. Data from Pb+Pb collisions at 158 A GeV. d/p^2 and \bar{d}/\bar{p}^2 yield ratios (left) and radii extracted from them (right), as a function of the number of participant nucleons N_p .

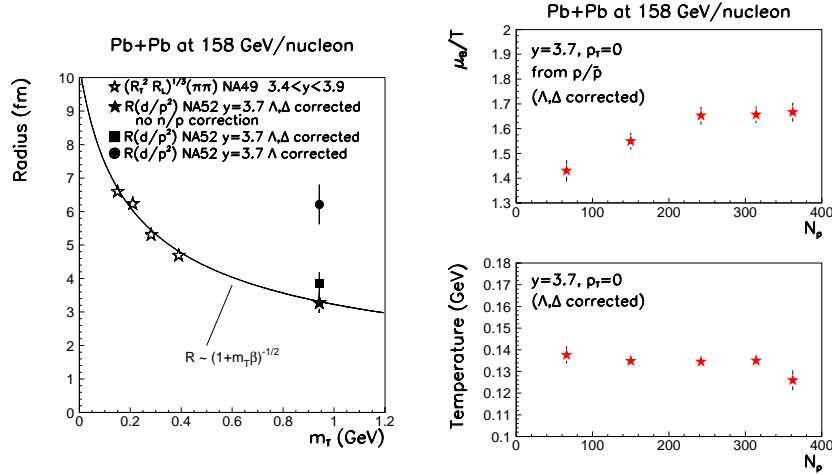


Fig. 5. Left: Transverse mass ($m_T = \sqrt{p_T^2 + m^2}$) dependence of the source radii extracted from d/p^2 at $y=3.7$ (full points, NA52 experiment) and of those extracted from $\pi\pi$ -correlations at $3.4 < y < 3.9$ (open points, NA49 experiment) in Pb+Pb collisions at 158 GeV per nucleon. Right: The baryochemical potential μ_B over the temperature T at $y=3.7$ and near zero p_T in Pb+Pb collisions at 158 A GeV, as a function of the mean number of participant nucleons.

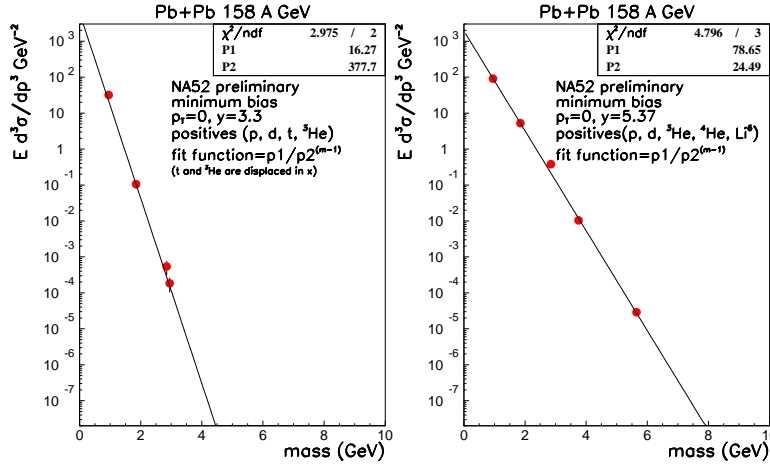


Fig. 6. Proton and nuclei cross sections as a function of mass in Pb+Pb collisions at 158 A GeV taken with a minimum bias trigger and near zero p_T . Left data at $y=3.3$ and right at $y=5.37$. The systematic errors have been quadratically added to the statistical ones. The resulting errorbars are of the size of the data points. The straight lines represent a fit through the data points using the function $f = p1/p2^{(m-1)}$.

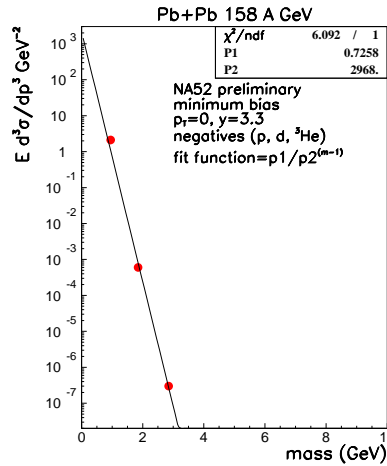


Fig. 7. Antiproton and antinuclei cross sections as a function of mass in Pb+Pb collisions at 158 A GeV taken with a minimum bias trigger and near zero p_T and at $y=3.3$. The systematic errors have been quadratically added to the statistical ones. The resulting errorbars are of the size of the data points. The straight lines represent a fit through the data points using the function $f = p1/p2^{(m-1)}$.

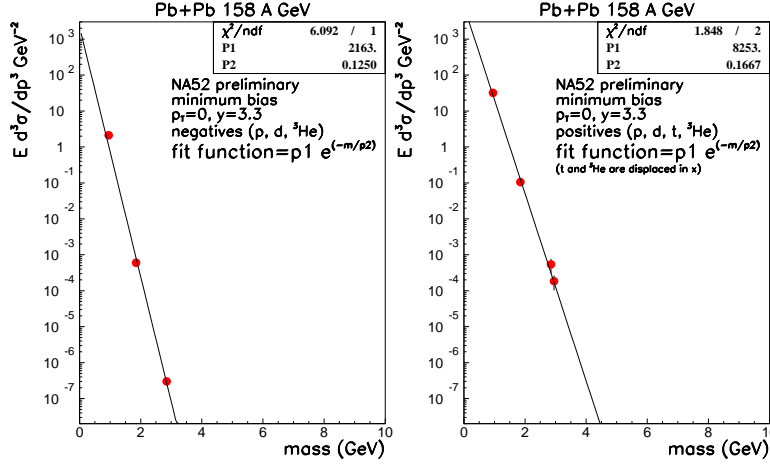


Fig. 8. Proton and nuclei (left) and antiproton and antinuclei (right) cross sections as a function of mass in Pb+Pb collisions at 158 A GeV taken with a minimum bias trigger, near zero p_T and at $y=3.3$. The systematic errors have been quadratically added to the statistical ones. The resulting errorbars are of the size of the data points. The straight lines represent a fit through the data points using the function $f = p1e^{(-m/T)}$.

In the comparison of the antiparticle to particle yields to the simple coalescence model prediction, as shown in figure 2, we assume that the positive and negative particles are produced through the same production mechanisms. We then examine whether this assumption is justified, by comparing the so called coalescence factors B_A for matter and antimatter. This factor is defined as

$$B_A = \frac{Y_A}{(Y_{\text{proton}})^A}$$

with A the atomic number and Y the invariant differential yields. Figure 3 shows the coalescence scaling factors for central and minimum bias events from the NA52 experiment together with other experimental data from the Bevalac [20, 21], BNL [22, 23, 24, 25] and the SPS [26] experiments. The NA52 coalescence scaling factors from d/p^2 and \bar{d}/\bar{p}^2 have been corrected for Λ and $\bar{\Lambda}$ decays.

Several observations can be made from figures 3:

Firstly, the coalescence factor is similar for matter and antimatter in accordance with the assumption that nuclei and antinuclei are produced through the same mechanism. It supports the description of coalescence production. Furthermore, the NA52 coalescence factors agree with data from the NA44 and NA49 experiments at the same trigger conditions, p_T and after the same weak decay corrections. The reduction of the coalescence factor with

increasing beam energy for heavy ion collisions, seen in figures 3 can be explained by an enhancement in the particle source volume due to expansion.

Secondly, the coalescence factors decrease with increasing centrality of the collisions. This can be due to an increase in the particle source volume, as more nucleons from the colliding nuclei are involved in the interaction. This tendency is also seen in figure 4 (left), where the coalescence factors B_2 and \overline{B}_2 as a function of the number of participant nucleons N are shown [7].

Under this assumption one can extract the volume of the particle source using a coalescence model [27]. The radii inferred from the d/p^2 and $\overline{d}/\overline{p}^2$ ratios increase with the number of participant nucleons N as $\sim N^{1/3}$, as shown in figure 4 (right) [7]. They are compared to the source radii obtained from $\pi\pi$ interferometry in Fig. 5 (left). The data are consistent with a transverse mass dependence of the source radii due to transverse expansion of the particle source [28].

Assuming chemical and thermal equilibrium for baryons and antibaryons we can infer from the measured particle yields information about the temperature T and baryochemical potential μ_b at the chemical freeze out. We assume that the particles fill the phase space according to a Boltzmann distribution. Thus we can write the invariant differential cross section for particles with a chemical potential μ , a spin S and an energy E as:

$$E \frac{d^3\sigma}{dp^3} = E \cdot (2S + 1) \cdot \sigma_{ppbb} \cdot \frac{V}{(2\pi)^3} \exp\left(-\frac{E - \mu}{T}\right) \quad (1)$$

Here V and T are the volume and temperature of the source, respectively.

In addition we assume that the volume and the temperature of the source is the same for all considered particles and that the chemical potentials of baryons (μ_b), antibaryons ($\mu_{\overline{b}}$) and nuclei (μ_A) are related as follows:

$$\mu_{\overline{b}} = -\mu_b \quad ; \quad \mu_A = A \cdot \mu_b. \quad (2)$$

From the cross section ratios of d/p , $\overline{d}/\overline{p}$ and \overline{p}/p we obtain μ_b and T . The latter parameters are shown in figure 5 (right), as a function of the mean number of participant nucleons in the collision [7]. We find that the temperature extracted using the ratios d/p , $\overline{d}/\overline{p}$ and \overline{p}/p , is ~ 125 MeV for the most central collisions. This temperature is the same as the one characterizing the thermal freeze-out of hadrons [29]. This finding supports the assumption that d and \overline{d} (and maybe \overline{p} too, as expected in [30]) freeze-out chemically, at the time of the thermal freeze-out of hadrons. It suggests that in pairs produced nuclei and antinuclei break up due to collisions in the phase between chemical and thermal freeze-out. Only the ones which form at a time close to thermal freeze-out of the other hadrons, have a chance to survive.

In Fig. 6 the production cross sections for baryons as a function of their mass are shown for central and forward rapidities $y=3.3$ and $y=5.7$ respectively. The data points are fit with a

function $f = p1/p2^{(m-1)}$ [31] from which the penalty in the production cross sections for higher mass nuclei can be extracted. The penalty factors f for positively charged baryons at midrapidity comes out to be $f=378$ per baryon, and at forward rapidity $f=24$. A similar fit to the antibaryon cross sections is shown in fig. 7. The obtained penalty factor is $f=2968$. The penalty factor for baryons is smaller than for antibaryons. This is due to the feeding of baryons from the fragmentation into the midrapidity region which is especially effective at low p_T . The penalty factors found in our experiment are different from the ones extracted from the AGS experiment E864 [31]. This is mainly due to the different energies of the incident ions and the different p_T acceptance of the detectors.

In figure 8 we compare the nuclei and antinuclei data with the expectation of a thermal model. The inverse slope parameter extracted from a fit with the function $f = p1e^{(-m/T)}$ through the antibaryon production cross sections at midrapidity turns out to give $T=125$ MeV (however the χ^2/DOF is not so good). The baryons at midrapidity however have a temperature of $T=167$ MeV (with a good χ^2/DOF). This difference is due to feeding from target and projectile fragments as described above. The temperature $T=125$ MeV found from the inverse slope parameter turns out to be consistent with the chemical freeze-out temperature obtained from the d/p , \bar{d}/\bar{p} and \bar{p}/p ratios and very close to the thermal freeze-out temperature $T=120$ MeV of other hadrons.

3. Summary

NA52 investigates particle and antiparticle production in Pb+Pb collisions at 158 A GeV. Two ${}^3\text{He}$ and 10^3 \bar{d} were observed. The decrease of the \bar{p}/p and the \bar{d}/d ratios with increasing centrality of the collision, suggests annihilation and breakup processes. The coalescence picture describes the Pb+Pb data well. The coalescence factors B_A decrease with increasing centrality of the collision due to an increasing source size. The extracted radius from the d/p^2 ratio is in agreement with pion interferometry results. The radii decrease with increasing m_T as expected for a transversally expanding source.

Using a thermal and a coalescence model we extract a thermal and a chemical freeze-out temperature for baryons and antibaryons of $T=125$ MeV. This temperature is very close to the thermal freeze-out temperature of hadrons at $T=120$ MeV. The results support the picture that the surviving nuclei and antinuclei are dominantly formed via coalescence at a time very close to the thermal freeze-out of hadrons, while those forming earlier are mostly destroyed due to annihilation and breakup reactions in the hadron dense environment.

Acknowledgements

We thank the Schweizerischer Nationalfonds for their support.

References

1. G. Appelquist et al., Phys. Rev. Lett. 76 (1996) 3907-3910.
2. F. Stoffel et al., APH N. S., Heavy Ion Physics 4 (1996) 429-434.
3. R. Klingenberg et al., Nucl. Phys. A 610 (1996) 306c-316c.
4. R. Klingenberg et al., Proceedings of the XXXII Rencontres de Moriond, QCD and High Energy Hadronic Interactions, 22-29 March 1997, Les Arc 1800, France, page 497.
5. M. Weber et al., Proceedings of the International Conference on Strangeness in Quark Matter, 20-25 July 2000, Berkeley, USA. To appear in J. Phys. G.
6. S. Kabana et al., Nucl. Phys. A 638 (1998) 411c-414c.
S. Kabana et al., J. of Phys. G 23 (1997) 2135.
7. M. Weber et al., Proceedings of the VII International Conference on Calorimetry in High Energy Physics, 9-14 Nov. 1997, Tucson, Arizona, USA.
S. Kabana et al., J. Phys. G: Nucl. Part. Phys. 25 (1999) 217-224.
S. Kabana et al., Nucl. Phys. A 661 (1999) 370c.
G. Ambrosini et al., New J. of Phys. 1, 22, 1999.
G. Ambrosini et al., New J. of Phys. 1, 23, 1999.
8. R. Arsenescu et al., J. Phys. G: Nucl. Part. Phys. 25 (1999) 225-233.
9. G. Ambrosini et al., Phys. Lett. B 417 (1998) 202-210.
10. G. Appelquist et al., Phys. Lett. B 376 (1996) 245-250.
11. M. Weber et al., Nucl. Phys. A 661 (1999) 177c.
12. G. Ambrosini et al., Proceedings of the International Conference on Strangeness in Quark Matter, 20-25 July 2000, Berkeley, USA. To appear in J. Phys. G. and hep-ph/0010053.
G. Ambrosini et al., paper submitted to the XXXth International Conference on High Energy Physics, 27 July-2 August 2000, Osaka, Japan, hep-ph/0010045.
13. K. Pretzl et al., Proceedings of the International Symposium on Strange and Quark Matter, Crete Hellas, Sept. 1994, edited by G. Vassiliadis, A. D. Panagiotou, B. S. Kumar and J. Madsen, World Scientific (1995) 230.
14. J. Ellis et al., Phys. Lett. B 233 (1989) 223.
S. Gavin et al., Phys. Lett. B 234 (1990) 175.
J. Schaffner et al., Z. Phys. A 341 (1991) 47.
15. CERN press release, 10 March 2000.
16. A. Jahns et al., Phys. Rev. Lett. 68 (1992) 19 2895.
St. Mrowczynski, Phys. Lett. B 308 (1993) 216.
M. Bleicher et al., Phys. Lett. B 361 (1995) 10.
17. S. Kabana, hep-ph/0010228, hep-ph/0010246, hep-ph/004138.
S. Kabana, P. Minkowski, hep-ph/0010247.
18. F. Sikler et al., (NA49 coll.) Nucl. Phys. A 661 (1999) p. 45.
19. W. Greiner, Int. Journal of Mod. Phys. E, Vol. 5, Nr. 1 (1995) 1-90.
20. S. Nagamiya et al., Phys. Rev. C 24 (1981) 971.
21. R. L. Auble et al., Phys. Rev. C 28 (1983) 1552.
22. N. Saito et al. (E886), Phys. Rev. C 49 (1994) 3211.

23. T. Abbott et al. (E802), Phys. Rev. C 50 (1994) 1024.
24. J. Barrette et al. (E814), Phys. Rev. C 50 (1994) 1077.
25. M. Aoki et al. (E858), Phys. Lett. B 69 (1992) 2345.
26. J. Simon-Gillo et al. (NA44), Nucl. Phys. A 590 (1995) 483c.
27. W.J. Llope et al., Phys. Rev. C 52, (1995) 4.
28. U. Heinz and R. Scheibl, nucl-th/9809092.
29. U. Heinz, Nuc. Phys. A 661, (1999) 141c.
30. R. Rapp, E. Shuryak, hep-ph/0008326.
31. J. Nagle et al., (E864 coll.), Nucl. Phys. A 661 (1999) 185c.
32. K. Werner, Phys. Rep. 232 (1993) 87.
33. A. Bussiere et al., Nucl. Phys. B 174 (1980) 1-15.